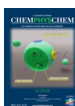


Special  
Issue

# Synthetic Ion Channels and DNA Logic Gates as Components of Molecular Robots

Ryuji Kawano\*<sup>[a]</sup>

A molecular robot is a next-generation biochemical machine that imitates the actions of microorganisms. It is made of biomaterials such as DNA, proteins, and lipids. Three prerequisites have been proposed for the construction of such a robot: sensors, intelligence, and actuators. This Minireview focuses on recent research on synthetic ion channels and DNA computing technologies, which are viewed as potential candidate components of molecular robots. Synthetic ion channels, which are embedded in artificial cell membranes (lipid bilayers), sense ambient ions or chemicals and import them. These artificial

sensors are useful components for molecular robots with bodies consisting of a lipid bilayer because they enable the interface between the inside and outside of the molecular robot to function as gates. After the signal molecules arrive inside the molecular robot, they can operate DNA logic gates, which perform computations. These functions will be integrated into the intelligence and sensor sections of molecular robots. Soon, these molecular machines will be able to be assembled to operate as a mass microrobot and play an active role in environmental monitoring and in vivo diagnosis or therapy.

## 1. Molecular Robots and the Lipid Bilayer Platform

Molecular robots have recently emerged based on biomolecules and biochemical processes. Approximately 30 years ago, a self-constructing machine, a so-called “assembler,” was originally proposed by Drexler.<sup>[1]</sup> Based on the idea of an assembler, molecular machines that operate autonomously have been developed using DNA or RNA. For example, DNA walkers move autonomously, on the basis of energy supplied from the hybridization of fuel oligonucleotides, from one binding site to another on a DNA-modified surface.<sup>[2,3]</sup> Rothemund has also proposed a method by which DNA molecules can be folded into any desired two-dimensional shape to make “DNA origami.”<sup>[4]</sup> In the field of synthetic chemistry, nanosized machines such as motors and ratchets have been developed based on organic or supramolecular chemistry.<sup>[5–7]</sup> This was viewed as ground-breaking technology and the pioneers have since been honored with the Nobel Prize in Chemistry 2016.

Inspired by the idea of a molecular assembler, molecular robotics, which involves construction with a much higher dimension of assembly, was proposed in 2014.<sup>[8]</sup> Molecular robots are composed of sensors, calculators, and actuators that are all implemented in liposomes or hydrogels. White blood cells, the most imageable example, senses the chemical signals secreted from a target bacterium, calculates the direction and length between the target and itself, and moves toward the signal

source by chemotaxis. These accomplished functions are integrated in a micron-sized body surrounded with a bilayer lipid membrane (BLM). Sato et al. reported the development of a sophisticated molecular robot prototype in 2017.<sup>[9]</sup> Their developed amoeba-type robot has light-induced DNA clutches for sensors and kinesin-microtubule proteins as actuators, all integrated in a cell-sized liposome. Light irradiation acts as a trigger for the release of the signal molecules and disengagement of the DNA clutches to change the shape of the liposome.

The fabrication process used for existing mechanical robots is viewed as a blueprint for the manufacture of these molecular robots. In the case of humanoid robots, the arms and legs are manufactured individually and then assembled. Similarly, individual fabrication would be a straightforward process in the manufacturing of molecular robots. Hence, a prototyping factory is required, as well as an industrial manufacturing process.

In this Minireview, I focus on manufacturing the body of the molecular robot using BLM with membrane receptors (Figure 1). BLM is the ideal material for the body of molecular robots because it is naturally biocompatible and can host receptor proteins. In addition, physical dynamics such as membrane fusion and endo- or exocytosis, such as molecular uptake processes, are useful for the interface of the robots. We previously developed a high-throughput planar BLM (pBLM) system that will be a powerful tool for the manufacturing of the lipid body of molecular robots.<sup>[10–12]</sup> A pBLM is generally used as the ion current measurement of an ion channel or pore-forming proteins. Because the reproducibility and stability of pBLMs are conventionally insufficient, various methods have been proposed to overcome this, primarily using microfluidic technology.<sup>[13]</sup> The most promising method is the droplet contact method,<sup>[14,15]</sup> in which two microdroplets surrounding the

[a] Dr. R. Kawano

Department of Biotechnology and Life Science  
Tokyo University of Agriculture and Technology (TUAT)  
2-24-16 Naka-cho, Koganei-shi, Tokyo 184-8588 (Japan)  
E-mail: rjkawano@cc.tuat.ac.jp

The ORCID identification number for the author of this article can be found under: <https://doi.org/10.1002/cphc.201700982>.

An invited contribution to a Special Issue on Reactions in Confined Spaces

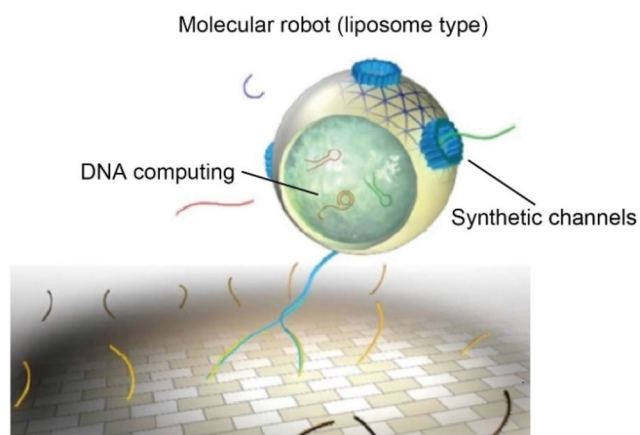


**Figure 1.** Conceptual illustration of a molecular robot. The body consists of a lipid bilayer with synthetic ion channels as the gate. DNA computing architecture is integrated inside the robot as the intelligence. (This illustration is used courtesy of Professor S. Murata of Tohoku University).

lipid monolayer are brought into contact and a stable and reproducible pBLM is formed at the droplet interface, as the droplet–interface bilayer. This method is simple and rapid, and the formed pBLM is extremely stable. Based on this method, several high-throughput pBLM formation methods have been proposed and applied to large-scale measurement of ion channels or nanopore measurements.<sup>[16–18]</sup>

In the following section, two recent efforts are introduced that attempted 1) to use a synthetic ion channel as the artificial receptor protein, and 2) autonomous sensing and calculation using DNA computing with nanopore technology using a high-throughput pBLM system. Synthetic channels are potential candidates for the sensor sections of molecular robots.

Ryuji Kawano was born in Oita, Japan in 1976. He received his Ph.D. in 2005 from Yokohama National University under the supervision of Prof. Masayoshi Watanabe, working on dye-sensitized solar cells using ionic liquid electrolytes and analyzing the charge transport mechanism using electrochemistry. Subsequently, he spent approximately three years in Prof.

Henry S. White's laboratory at the University of Utah as a postdoctoral researcher, where he conducted research on nanopore measurements with glass materials. He then joined Prof. Shoji Takeuchi's group at the Kanagawa Academy of Science and Technology (KAST) and University of Tokyo, where he carried out research on the construction of durable lipid bilayer systems using microfabricated devices. Since 2014, he has been working as an Associate Professor (tenure-track) at Tokyo University of Agriculture and Technology. His current research interests include molecular robotics based on synthetic membrane proteins, DNA computing, and nanopore technology based on microfabrication.



DNA computing technology with nanopore proteins will be able to connect the sensor and intelligence functions.

## 2. Synthetic Ion Channels and Transport Control at the Lipid Bilayer Membrane

Receptor proteins sense specific molecules in the cell membrane. When the ligand molecule binds to a receptor, the receptor senses the binding and produces a signal that is transmitted downstream to control ion transport through ion channels, as it cascades. Furthermore, pore-forming proteins play a key role in the transportation of molecules with the gradient of membrane potential or the substrate concentration. Artificial ion channels or pores have been created using synthetic chemistry to mimic the structure or function of natural proteins.<sup>[19,20]</sup> In the last three decades, synthetic chemists have proposed various compounds that actively exhibit ion channel structures and functions.<sup>[21]</sup> As part of the design, chemists try to add functions such as pore size, ion or substrate selectivity, and voltage or ligand gating. In the early studies, researchers imitated natural compounds, such as valinomycin or gramicidin, for the structural framework of synthetic channels (Figure 2a). Valinomycin is a macrocyclic polypeptide used in the transport of potassium, as an antimicrobial peptide. Gramicidin is also a polypeptide and forms a  $\beta$ -helix structure in the lipid monolayer,<sup>[22]</sup> within the bilayer, two gramicidin molecules form an end-to-end dimer, which in turn forms a transmembrane structure in the bilayer. These macrocyclic or dimer structures have been modeled for the design of synthetic channels, and chemists synthesized the mimicking structure using synthetic peptides or macromolecules. More recently, other functional materials such as DNA origami and carbon nanotubes have been proposed as potential candidates for artificial ion channels.<sup>[19,23,24]</sup>

One of the most sought after properties is ion selectivity for  $\text{Na}^+$ ,  $\text{K}^+$ ,  $\text{Ca}^{2+}$ ,  $\text{Cl}^-$ , and other ions. Most studies have focused on synthesis of the channel structure in the lipid membrane, and assessed the ion selectivity. Among them, the first report of a selective channel was for  $\text{K}^+$  ions.<sup>[25]</sup> In nature, potassium-channel proteins use a selective filter that has five amino acids, TVGYG, within each of the four subunits. The hydrated  $\text{K}^+$  ion is dehydrated by interacting with these motifs, and then passes through the filter pore with high ion selectivity (Figure 2b).<sup>[26]</sup> Conversely, in the synthetic channels, the  $\text{K}^+$ -selective filter is composed of an aromatic ring (primarily formed by four tyrosine residues) that provides a weak electric field, allowing complete dehydration of  $\text{K}^+$  ions, but not of  $\text{Na}^+$  ions.

In this system, the  $\pi$  electrons of the aromatic rings contribute to the lowering of the potential barrier for passage of  $\text{K}^+$  ions through attractive  $\pi$ -cation interactions (Figure 2c).<sup>[20]</sup> Following examination of  $\text{K}^+$  selectivity, the selection trend, for example,  $\text{Li}^+ > \text{Na}^+ > \text{K}^+$ , is estimated in terms of alkali metal ions, as the Eisenman sequence.<sup>[27]</sup> The selectivity for other ions or molecules, such as halide ions, divalent ions, and ammonium ions has also been studied extensively by researchers. More recently, a de novo strategy from protein engineering

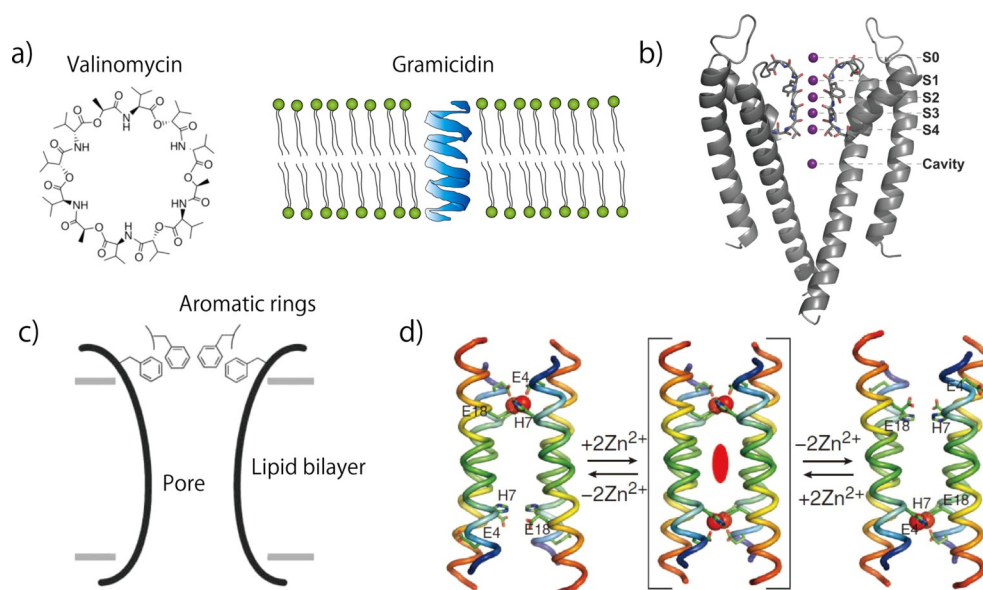


**Figure 2.** Natural and synthetic ion channels. a) Structures of valinomycin and gramicidin. Gramicidin is a toxin channel and forms a transmembrane structure by dimerization.<sup>[22]</sup> b) Structure of the  $K^+$ -selective filter of the KcsA channel (deposited in the Protein Data Bank under accession no. 1K4C). The side chain of the amino acid residue threonine of the signature sequence is shown because it participates in coordinating a  $K^+$  ion at site S4.<sup>[26]</sup> c) Schematic representation of the selective filter of a general synthetic channel. The filter consists of aromatic rings and cation- $\pi$  interactions are important for selectivity.<sup>[20]</sup> Reproduced with permission from Ref. [20]. Copyright (2006) Royal Society of Chemistry. d) Structure of a transmembrane  $Zn^{2+}$ -selective channel, which consists of four-helix bundles of de novo designed short polypeptides.<sup>[28]</sup> Reproduced with permission from Ref. [28]. Copyright (2014) The American Association for the Advancement of Science.

has become a powerful tool for designing ion-selective peptide channels. DeGrado and co-workers reported on the design of a membrane-spanning, four-helical bundle peptide that transports  $Zn^{2+}$  and  $Co^{2+}$  ions, but not  $Ca^{2+}$ , across membranes (Figure 2d).<sup>[28]</sup>

Other challenging directions of synthetic channel studies are active transportation (pumping) and control of open-close states (gating). Although these two properties (i.e., pumping and gating) are suitable for imitating natural ion channels, the strategies of the imitation are still being explored. In the context of pumping, the transport of ions across membranes and against a thermodynamic gradient is essential to many biological processes. Gust et al. proposed a strategy for photo-induced  $Ca^{2+}$  ion transport via lipid membranes.<sup>[29]</sup> The proposed strategy uses a synthetic, light-driven transmembrane  $Ca^{2+}$  pump based on a redox-sensitive lipophilic  $Ca^{2+}$ -binding shuttle molecule powered by an intramembrane artificial photosynthetic reaction center (Figure 3a). The active transport is driven not by concentration gradients, but by light-induced electron transfer in a photoactive center that is asymmetrically disposed across a lipid bilayer. Photoswitchable molecules for manipulating ion channels have also been proposed by Trauner and Feringa.<sup>[30,31]</sup> Other interesting strategies based on electron transfer with a redox reaction have also been proposed. Stoddart and co-workers synthesized a wholly artificial supermolecule that acts on small molecules to create a gradient in their local concentration (Figure 3b).<sup>[32]</sup> This enables a redox-active ring viologen to move along an oligomethylene axis as the redox reactions proceed. In experiments conducted, the artificial pump operated reversibly for two cycles of opera-

tion and drove rings against the concentration gradient, but the system did not conduct movement in the lipid membrane.

Controlling the open-close state (gating) of synthetic channels, by contrast, is very challenging. Most approaches utilize voltage gating: an early approach used by Fyles and co-workers<sup>[33]</sup> and Kobuke and co-workers<sup>[34]</sup> involved an asymmetrical structure with charged parts at one of the termini in the transmembrane molecules. Kawano, Furukawa and co-workers have also attempted to create gating-controllable synthetic channels.<sup>[35]</sup> They focused on metal-organic scaffolds because of the tunability of the structure.<sup>[36]</sup> Metal-organic frameworks have attracted substantial attention as porous materials, especially for adsorption or storage of gas molecules. Recently, Kim and co-workers<sup>[37]</sup> investigated the capability of metal-organic molecules as synthetic ion channels. Following their study, we synthesized rhodium metal-organic polyhedrals (RhMOPs) that have two different lengths of alkoxy chains ( $C_{12}$  and  $C_{14}$ ) at the periphery for controlling the open-close state, called  $C_{12}$ RhMOP and  $C_{14}$ RhMOP.<sup>[35]</sup> In addition, these RhMOP molecules showed two distinct channel conductance states because the Archimedean geometry of the MOP structure allows porous molecules to possess more than two different polygonal apertures and one internal cavity (Figure 3c). Therefore, ions pass through the internal cavity of the RhMOP via either the square or the triangular aperture exposed to the aqueous phase in the lipid bilayer. The long alkoxy chains at the periphery can facilitate interaction with lipid molecules, and the difference in the length enables modulation of its interaction such that it can alter the molecular dynamics, resulting in switching between the open-close states.

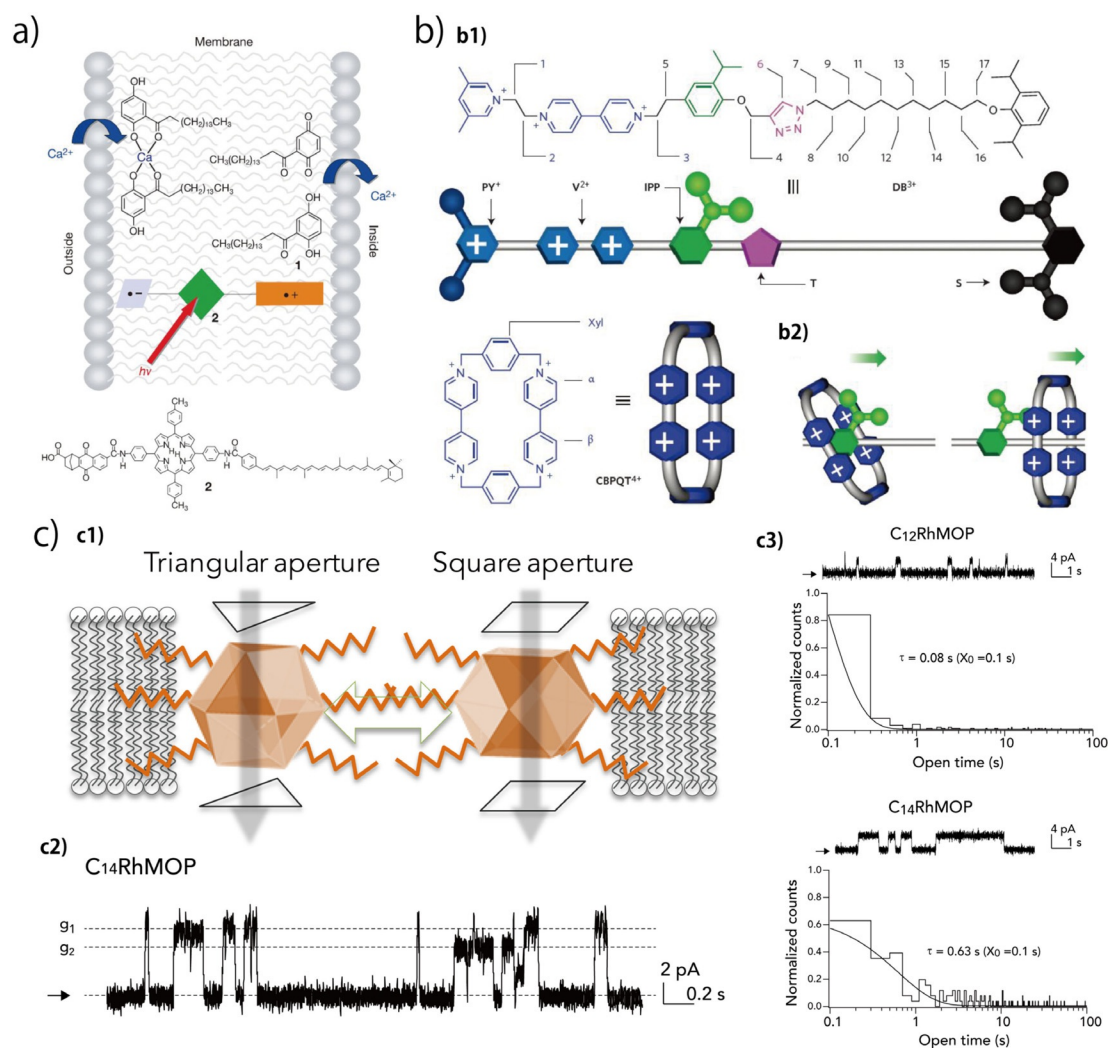


**Figure 3.** Synthetic ion channels with particular functions. a) Schematic illustration of a light-powered transmembrane  $\text{Ca}^{2+}$  pump system.<sup>[29]</sup> Reproduced with permission from Ref. [29]. Copyright (2002) Nature Publishing Group. b) Structure and schematic illustration of the molecular pump that operates the redox reaction.<sup>[32]</sup> Reproduced with permission from Ref. [32]. Copyright (2015) Nature Publishing Group. c1) Schematic illustration and channel signals of the open–close state of the MOP channel. c2) The multiple conductance states observed from a single molecule. c3) The open-channel state (duration) can be controlled by changing the outer structure.<sup>[35]</sup> Reproduced with permission from Ref. [35]. Copyright (2017) Elsevier.

As described above, synthetic channels will be useful tools at the interface of the molecular robots and their external environment. This is because the selectivity of information, as ions or molecules, and controllability of the gating are absolutely imperative. The next step is regulation of these functions from external stimulation using light irradiation, magnetic fields, or electrical stimulation.

### 3. Nanopore Technology Meets DNA Computing and is Applied to Practical Sensing

Nanopores—pore-forming transmembrane proteins—are another strong candidate for the sensors of molecular robots. Sensing with nanopores has emerged as a method for single-molecule detection.<sup>[38,39]</sup> This method works by applying an electric potential that causes single molecules to be passed through the nanopore. The change in the ionic current over time is recorded, potentially allowing the direct collection of

information about individual molecules in terms of size and mobility (Figure 4a). Although this method can detect single molecules, the selectivity relies on the size compatibility between the nanopore and target molecules. An  $\alpha$ -hemolysin ( $\alpha\text{HL}$ ), pore-forming toxin from *Staphylococcus aureus*, is commonly used as the biological nanopore. This protein has a 1.4 nm diameter pore that allows single-stranded DNA (ssDNA) to pass but blocks double-strand DNA (dsDNA), suggesting that the nanopore has precise size selectivity for DNA/RNA detection.<sup>[40,41]</sup> For the detection of smaller molecules, a molecular adapter such as cyclodextrin, which reduces the pore size, has been used (Figure 4b).<sup>[42,43]</sup> DNA aptamers have also been applied as the molecular tag for selective detection because  $\alpha\text{HL}$  cannot detect larger sized molecules (Figure 4c).<sup>[18]</sup> Conversely, we have studied much larger nanopores from five different protein families for precise nanopore detection.<sup>[44]</sup> Recently, a promising application of nanopore measurements for DNA sequencing has also resulted from ardent efforts, with a

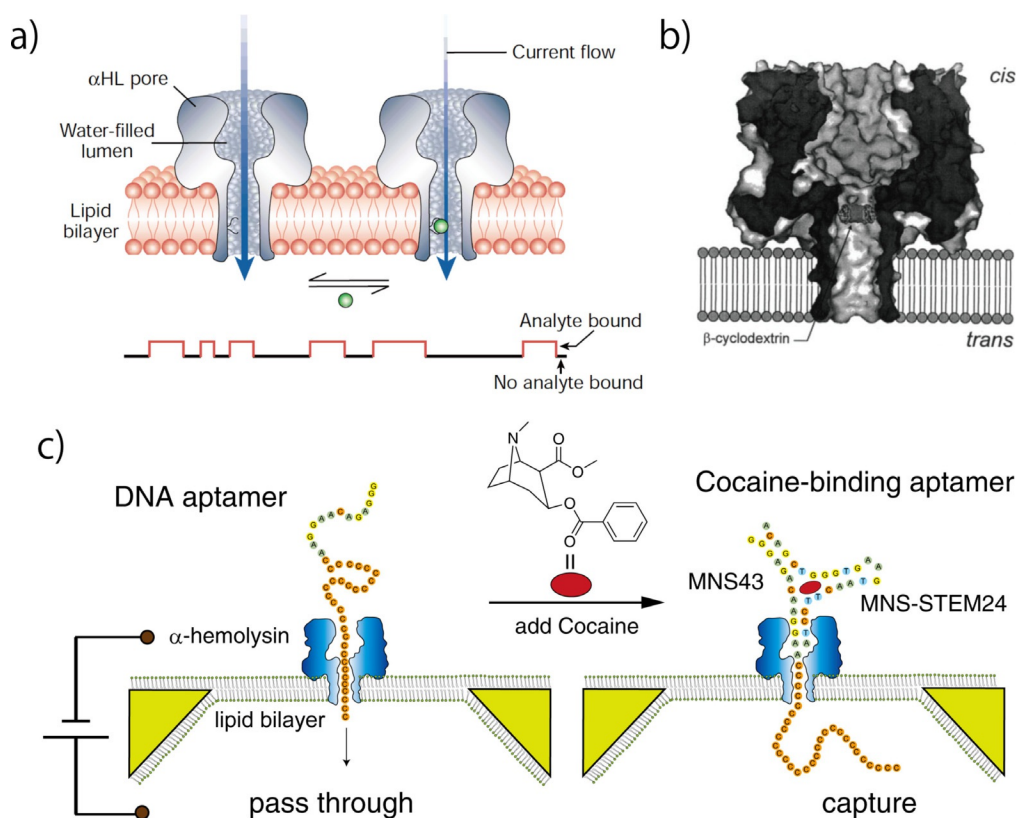


**Figure 4.** Nanopore measurements. a) Conceptual illustration of nanopore sensing.<sup>[39]</sup> Reproduced with permission from Ref. [35]. Copyright (2017) Elsevier. b) A cyclodextrin embedded in an  $\alpha$ HL pore operates as the adapter for detecting small molecules.<sup>[42,43]</sup> Reproduced with permission from Ref. [43]. Copyright (2000) Elsevier. c) DNA aptamers are also used for selective detection of small molecules.<sup>[18]</sup> In the absence of target molecules, the aptamer is a ssDNA and passes through the pore. In the presence of the target, the DNA aptamer binds it and forms a complex, which cannot pass through the pore, generating characteristic current signals. Reproduced with permission from Ref. [18]. Copyright (2011) The American Chemical Society.

nanopore sequencer being commercialized in 2015. To this end, because conventional nanopores are highly compatible for detecting oligonucleotides, we have attempted to integrate the nanopore method into DNA computing in order to connect the sensoria and the intelligence of the molecular robots.

We have attempted to perform NAND logic calculations in a four-droplet system and to detect the output DNA molecule using an  $\alpha$ HL nanopore reconstituted in the droplet-interface bilayer (Figure 5a).<sup>[45]</sup> This droplet system has two inputs, an operation droplet for calculations, and an output droplet. After calculating the two input DNAs, they pass through the  $\alpha$ HL nanopore and are transferred from the calculation to the output droplet. In this operation, ssDNA translocation through the  $\alpha$ HL nanopore signifies an output of 1, whereas absence of DNA translocation signifies an output of 0. Output DNA molecules are detected by  $\alpha$ HL nanopores with single-molecule translocation, and the system was label-free. The operation is relatively faster (approximately 10 min) than the conventional method. Next, we attempted to integrate more complex operations into this nanopore-droplet system. This system functions as an AND gate with amplification and transcription from DNA to RNA, using T7 RNA polymerase (T7RP).<sup>[46]</sup> To construct this system, we used two input DNAs and template DNA containing part of the T7RP promoter region, as shown in Figure 5b. For cases in which two input DNAs exist, defined as input (1 1),

the two DNAs form a duplex that hybridizes with the template DNA. The T7RP polymerase binds to the promoter region and synthesizes a large amount of RNA as output 1. In the cases of inputs (0 0), (0 1), and (1 0), the input DNA cannot hybridize with the template DNA, resulting in an output of 0. In addition, this AND gate operation was simultaneously conducted using a parallel droplet device with a short period (Figure 5c). Integration of DNA logic gates into electrochemical devices is important to ensure that molecules containing output information, such as diagnostic results, can be processed as human-recognizable information. In the next step, the programmable system is applied to practical application, for example, cancer diagnosis using microRNA.

MicroRNAs (miRNAs) are noncoding, small, single-stranded RNAs. They are involved in the regulation of over 60% of human genes, and they play significant roles in physiological processes.<sup>[47]</sup> Accumulated evidence has revealed that aberrant levels of miRNA expression in tissues or blood is associated with various human diseases such as cancers and cardiovascular diseases. Therefore, miRNA is an emerging class of clinically important biomarkers for early diagnosis. A landmark report on miRNA detection using  $\alpha$ HL nanopore was presented by Gu and co-workers. They used an oligonucleotide probe that binds to the target miRNA and generates programmable current signatures in the nanopore measurements (Figure 6a).<sup>[48]</sup>

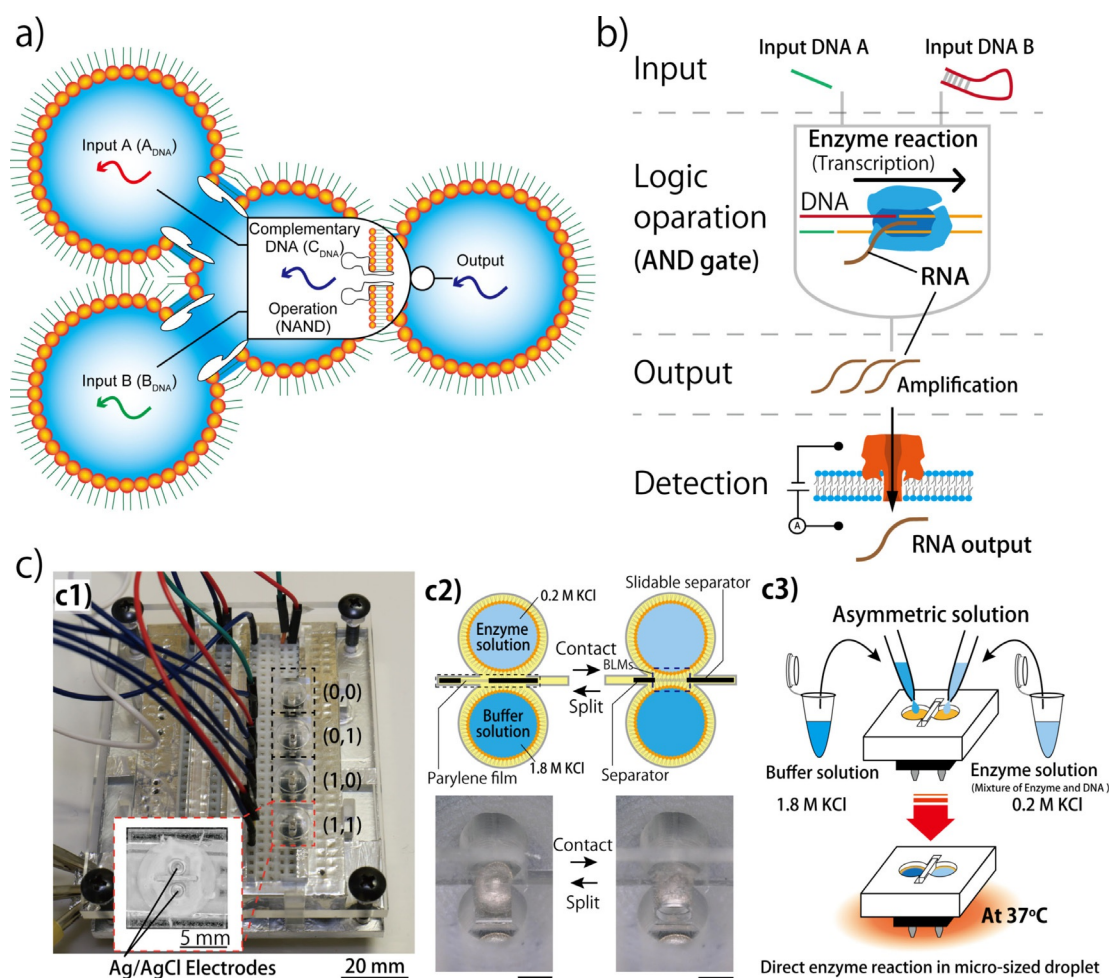


**Figure 5.** DNA logic gate integrated into the droplet bilayer system. a) NAND operation system with four droplet networks comprising two input, one operation, and one output droplet.<sup>[45]</sup> b) DNA to RNA transcription AND gate using an enzymatic reaction.<sup>[46]</sup> Reproduced with permission from Ref. [46]. Copyright (2017) The American Chemical Society. c) Transcription AND operation performed in parallel with the droplet device. c1) Photograph of the device. c2) The operation with the enzyme-catalyzed reaction can be implemented in the droplet. c3) The asymmetric two-solution (buffer-enzyme) condition is key to the enzymatic reaction and nanopore measurement. Reproduced with permission from Ref. [46]. Copyright (2017) The American Chemical Society.

Using this system, they were able to selectively detect miRNAs at sub-picomolar levels in samples obtained from lung cancer patients. Subsequently, they applied the method to multiple miRNA detection by using DNA and polyethylene glycol tags as the barcode.<sup>[49]</sup> The system also represented the programmable nanopore currents from four lung-cancer-derived miRNAs. We also proposed a theranostics system, which involves the combination of diagnosis and therapy at the same time, using a nanopore-droplet device (Figure 6b).<sup>[50]</sup> The proposed system includes autonomous diagnosis of cancers using miRNA (as the input molecule) and therapy for the tumor cells by a DNA antisense drug (as the output molecule). In the presence of miR-20a secreted from a small-cell lung cancer (SCLC), two programmable DNAs functioning as diagnostic molecules bind to the input miR-20a, and form a three-way junction structure. At that time, isothermal reactions with enzymes (a Klenow fragment as the polymerase and Nt.AlwI as the nicking enzyme) repeatedly occur to generate a DNA drug called oblimersen. The generated molecules were quantified by the translocation frequency of the nanopore measurement in real

time (Figure 6c). The results of nanopore quantification showed that oblimersen was amplified more than 20-fold from the input miR-20a, which meets the dosage requirement for SCLC therapy. Based on these DNA computing techniques, we have recently reported an approach for detection of miRNA at ultra-low concentrations, in which the target miRNA is amplified from 1 fM to pM level and then nanopores with asymmetrical electrolyte condition are detected, which can increase the event frequency of miRNA translocation.<sup>[51]</sup>

Combining nanopore and DNA computing technologies is useful for constructing smart and autonomous sensing at the interface region. The nanopore/DNA computing system will contribute to the construction of intelligent sensors for molecular robots.

#### 4. Perspectives for Molecular Robots with Lipid Bilayers

This Minireview focused on functionalization of lipid bilayers embedded with synthetic ion channels or nanopores with DNA

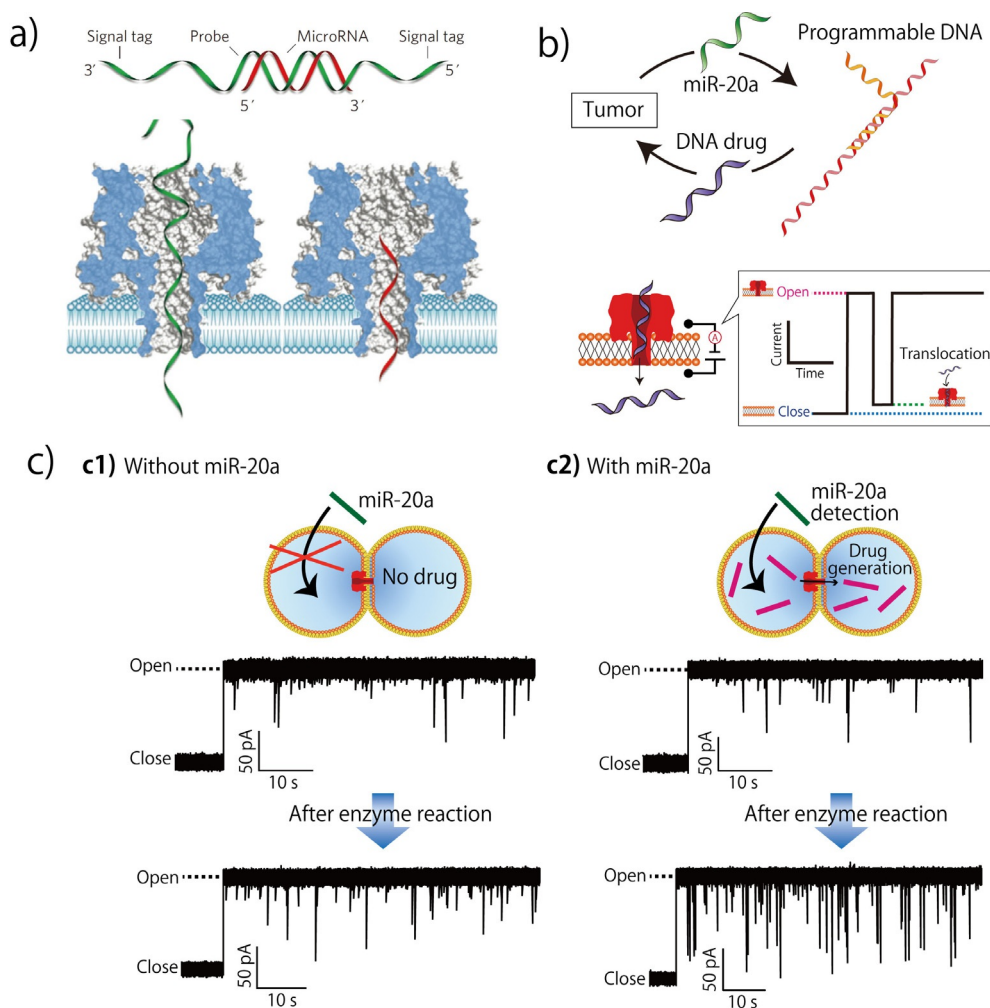


**Figure 6.** MicroRNA (miRNA) detection using a nanopore. a) A molecular tag is useful for generating a characteristic signal current.<sup>[48]</sup> Reproduced with permission from Ref. [48]. Copyright (2011) Nature Publishing Group. b) A theranostic system for a small-cell lung cancer. If miR-20a is detected, programmable DNA molecules autonomously generate the DNA antisense drug for therapy of the cancer. Reproduced with permission from Ref. [50]. Copyright (2017) The American Chemical Society. c) A nanopore can estimate and generate the DNA drug without (c1) or with (c2) miR-20a in real time.<sup>[50]</sup> Reproduced with permission from Ref. [50]. Copyright (2017) The American Chemical Society.

logic operation. These functions or technologies of such molecular machines and autonomous systems have matured sufficiently that they can operate on their own. Regarding the synthetic ion channels, early studies focused on constructing a transmembrane structure mimicking natural ion channels. Then, the transport properties such as ion selectivity or gating probability were investigated. Although in most cases the functions were carried out in a single operation, the natural ion channels work in signal cascades, and ion transport can induce a biological reaction. In the next step, the synthetic ion channel will be loaded onto the interface of the molecular robot. DNA logic operations face a similar situation. Single operations such as AND, OR, and NAND can be combined to make sophisticated systems. Therefore, recent compelling work has shown that combining nanopore and DNA logic operations can result in a system that can be integrated into the body and interface with molecular robots.

Similar approaches can be found in synthetic biology and protocell studies, in which biological technologies such as

gene manufacturing are used. It is envisaged that by fusing these technologies and science, in the future, microorganisms such as molecular robots will operate in living systems for diagnosis and therapy, in other environments for assessment or recovery, and in space for terraforming.

## Acknowledgements

I wish to thank Professor Satoshi Murata of Tohoku University for providing the beautiful illustration of a molecular robot (Figure 1). This research was supported in part by KAKENHI, "Molecular Robotics" (Grant No. 15H00803), and MEXT, Japan (Grant No. 16H06043).

## Conflict of Interest

The author declares no conflict of interest.

**Keywords:** DNA computing · lipids · molecular robots · nanopores · synthetic ion channels

- [1] K. E. Drexler, *Proc. Natl. Acad. Sci. USA* **1981**, *78*, 5275–5278.
- [2] K. Lund, A. J. Manzo, N. Dabby, N. Michelotti, A. Johnson-Buck, J. Nangreave, S. Taylor, R. J. Pei, M. N. Stojanovic, N. G. Walter, E. Winfree, H. Yan, *Nature* **2010**, *465*, 206–210.
- [3] F. C. Simmel, *Curr. Opin. Biotechnol.* **2012**, *23*, 516–521.
- [4] P. W. K. Rothemund, *Nature* **2006**, *440*, 297–302.
- [5] J. P. Sauvage, *Acc. Chem. Res.* **1998**, *31*, 611–619.
- [6] W. R. Browne, B. L. Feringa, *Nat. Nanotechnol.* **2006**, *1*, 25–35.
- [7] V. Balzani, A. Credi, F. M. Raymo, J. F. Stoddart, *Angew. Chem. Int. Ed.* **2000**, *39*, 3348–3391; *Angew. Chem.* **2000**, *112*, 3484–3530.
- [8] M. Hagiya, A. Konagaya, S. Kobayashi, H. Saito, S. Murata, *Acc. Chem. Res.* **2014**, *47*, 1681–1690.
- [9] Y. Sato, Y. Hiratsuka, I. Kawamata, S. Murata, S. M. Nomura, *Science Robotics* **2017**, *2*, eaal3735.
- [10] R. Kawano, Y. Tsuji, K. Sato, T. Osaki, K. Kamiya, M. Hirano, T. Ide, N. Miki, S. Takeuchi, *Sci. Rep.* **2013**, *3*, 1995.
- [11] H. Watanabe, R. Kawano, *Anal. Sci.* **2016**, *32*, 57–60.
- [12] M. Ohara, Y. Sekiya, R. Kawano, *Electrochem.* **2016**, *84*, 338–341.
- [13] M. Zagnoni, *Lab Chip* **2012**, *12*, 1026–1039.
- [14] K. Funakoshi, H. Suzuki, S. Takeuchi, *Anal. Chem.* **2006**, *78*, 8169–8174.
- [15] M. A. Holden, D. Needham, H. Bayley, *J. Am. Chem. Soc.* **2007**, *129*, 8650–8655.
- [16] R. Syeda, M. A. Holden, W. L. Hwang, H. Bayley, *J. Am. Chem. Soc.* **2008**, *130*, 15543–15548.
- [17] A. M. El-Arabi, C. S. Salazar, J. J. Schmidt, *Lab Chip* **2012**, *12*, 2409–2413.
- [18] R. Kawano, T. Osaki, H. Sasaki, M. Takinoue, S. Yoshizawa, S. Takeuchi, *J. Am. Chem. Soc.* **2011**, *133*, 8474–8477.
- [19] N. Sakai, S. Matile, *Langmuir* **2013**, *29*, 9031–9040.
- [20] A. L. Sisson, M. R. Shah, S. Bhosale, S. Matile, *Chem. Soc. Rev.* **2006**, *35*, 1269–1286.
- [21] J. K. W. Chui, T. M. Fyles, *Chem. Soc. Rev.* **2012**, *41*, 148–175.
- [22] G. A. Woolley, B. A. Wallace, *J. Membr. Biol.* **1992**, *129*, 109–136.
- [23] J. Geng, K. Kim, J. F. Zhang, A. Escalada, R. Tunuguntla, L. R. Comolli, F. I. Allen, A. V. Shnyrova, K. R. Cho, D. Munoz, Y. M. Wang, C. P. Grigoropoulos, C. M. Ajo-Franklin, V. A. Frolov, A. Noy, *Nature* **2014**, *514*, 612–615.
- [24] M. Langecker, V. Arnaut, T. G. Martin, J. List, S. Renner, M. Mayer, H. Dietz, F. C. Simmel, *Science* **2012**, *338*, 932–936.
- [25] Y. Tanaka, Y. Kobuke, M. Sokabe, *Angew. Chem. Int. Ed. Engl.* **1995**, *34*, 693–694; *Angew. Chem.* **1995**, *107*, 717–719.
- [26] E. Gouaux, R. MacKinnon, *Science* **2005**, *310*, 1461–1465.
- [27] G. Eisenman, R. Horn, *J. Membr. Biol.* **1983**, *76*, 197–225.
- [28] N. H. Joh, T. Wang, M. P. Bhate, R. Acharya, Y. B. Wu, M. Grabe, M. Hong, G. Grigoryan, W. F. DeGrado, *Science* **2014**, *346*, 1520–1524.
- [29] I. M. Bennett, H. M. V. Farfano, F. Bogani, A. Primak, P. A. Liddell, L. Otero, L. Sereno, J. J. Silber, A. L. Moore, T. A. Moore, D. Gust, *Nature* **2002**, *420*, 398–401.
- [30] M. Banghart, K. Borges, E. Isacoff, D. Trauner, R. H. Kramer, *Nat. Neurosci.* **2004**, *7*, 1381–1386.
- [31] W. Szymański, D. Yilmaz, A. Kocer, B. L. Feringa, *Acc. Chem. Res.* **2013**, *46*, 2910–2923.
- [32] C. Y. Cheng, P. R. McGonigal, S. T. Schneebeli, H. Li, N. A. Vermeulen, C. F. Ke, J. F. Stoddart, *Nat. Nanotechnol.* **2015**, *10*, 547–553.
- [33] T. M. Fyles, D. Loock, X. Zhou, *Can. J. Chem.* **1998**, *76*, 1015–1026.
- [34] Y. Kobuke, K. Ueda, M. Sokabe, *J. Am. Chem. Soc.* **1992**, *114*, 7618–7622.
- [35] R. Kawano, N. Horike, Y. Hijikata, M. Kondo, A. Carne-Sanchez, P. Larpent, S. Ikemura, T. Osaki, K. Kamiya, S. Kitagawa, S. Takeuchi, S. Furukawa, *Chem* **2017**, *2*, 393–403.
- [36] S. Furukawa, J. Reboul, S. Diring, K. Sumida, S. Kitagawa, *Chem. Soc. Rev.* **2014**, *43*, 5700–5734.
- [37] M. Jung, H. Kim, K. Baek, K. Kim, *Angew. Chem. Int. Ed.* **2008**, *47*, 5755–5757; *Angew. Chem.* **2008**, *120*, 5839–5841.
- [38] S. Howorka, Z. Siwy, *Chem. Soc. Rev.* **2009**, *38*, 2360–2384.
- [39] H. Bayley, P. S. Cremer, *Nature* **2001**, *413*, 226–230.
- [40] J. J. Kasianowicz, E. Brandin, D. Branton, D. W. Deamer, *Proc. Natl. Acad. Sci. USA* **1996**, *93*, 13770–13773.
- [41] D. Branton, D. W. Deamer, A. Marziali, H. Bayley, S. A. Benner, T. Butler, M. Di Ventra, S. Garaj, A. Hibbs, X. H. Huang, S. B. Jovanovich, P. S. Krstic, S. Lindsay, X. S. Ling, C. H. Mastrangelo, A. Meller, J. S. Oliver, Y. V. Pershin, J. M. Ramsey, R. Riehn, G. V. Soni, V. Tabard-Cossa, M. Wanunu, M. Wiggin, J. A. Schloss, *Nat. Biotechnol.* **2008**, *26*, 1146–1153.
- [42] L. Q. Gu, O. Braha, S. Conlan, S. Cheley, H. Bayley, *Nature* **1999**, *398*, 686–690.
- [43] L. Q. Gu, H. Bayley, *Biophys. J.* **2000**, *79*, 1967–1975.
- [44] H. Watanabe, A. Gubbiotti, M. Chinappi, N. Takai, K. Tanaka, K. Tsumoto, R. Kawano, *Anal. Chem.* **2017**, *89*, 11269–11277.
- [45] H. Yasuga, R. Kawano, M. Takinoue, Y. Tsuji, T. Osaki, K. Kamiya, N. Miki, S. Takeuchi, *PLoS One* **2016**, *11*, e0149667.
- [46] M. Ohara, M. Takinoue, R. Kawano, *ACS Synth. Biol.* **2017**, *6*, 1427–1432.
- [47] C. M. Croce, *Nat. Rev. Genet.* **2009**, *10*, 704–714.
- [48] Y. Wang, D. L. Zheng, Q. L. Tan, M. X. Wang, L. Q. Gu, *Nat. Nanotechnol.* **2011**, *6*, 668–674.
- [49] X. Y. Zhang, Y. Wang, B. L. Fricke, L. Q. Gu, *ACS Nano* **2014**, *8*, 3444–3450.
- [50] M. Hiratani, M. Ohara, R. Kawano, *Anal. Chem.* **2017**, *89*, 2312–2317.
- [51] H. Zhang, M. Hiratani, K. Nagaoka, R. Kawano, *Nanoscale* **2017**, *9*, 16124–16127.

Manuscript received: September 5, 2017

Accepted manuscript online: November 10, 2017

Version of record online: December 8, 2017